Hyperfine Interact (2018) 239: 11
https://doi.org/10.1007/s10751-018-1488-0

^{61}Ni synchrotron-radiation-based Mössbauer absorption spectroscopy of Ni nanoparticle composites

Ryo Masuda[1] · **Hirokazu Kobayashi**[2,3] · **Yoshimasa Aoyama**[2] · **Makina Saito**[1] · **Shinji Kitao**[1] · **Hiroki Ishibashi**[1] · **Shuichi Hosokawa**[1] · **Takaya Mitsui**[4] · **Yoshitaka Yoda**[5] · **Hiroshi Kitagawa**[2] · **Makoto Seto**[1,4]

Abstract We obtained energy-domain ^{61}Ni synchrotron-radiation-based Mössbauer absorption spectra of three materials that relate to nanoparticles: $Ni_2(C_8O_6H_2)$ metal-organic frameworks (MOFs), Ni nanoparticles synthesized by complete heat decomposition of the MOFs, and the composites of Ni nanoparticles and the MOFs synthesized by partial decomposition of the MOFs. The ^{61}Ni abundance of all the samples was not enriched but we were successfully able to obtain their spectra in 1 day or less, by using a highly efficient measurement system where the internal conversion electrons from energy standard $^{61}Ni_{86}V_{14}$ foil were detected. Although both nanoparticle constituent and MOF constituent in the composites included Ni atoms, the Mössbauer parameters of the Ni nanoparticle constituent could be evaluated; the magnetic hyperfine field of the Ni nanoparticle constituent in the composites was different from that of the Ni nanoparticles obtained by the complete heat decomposition. This difference implied that the 3*d* and/or 4*s* electron configuration of the nanoparticle constituent were affected by the MOF constituent in the composites.

This article is part of the Topical Collection on *Proceedings of the International Conference on the Applications of the Mössbauer Effect (ICAME 2017), Saint-Petersburg, Russia, 3–8 September 2017*
Edited by Valentin Semenov

✉ Ryo Masuda
masudar@rri.kyoto-u.ac.jp

[1] Research Reactor Institute, Kyoto University, Kumatori-cho, Sennan-gun, Osaka 590-0494, Japan

[2] Division of Chemistry, Graduate School of Science, Kyoto University, Kyoto, 606-8502, Japan

[3] Precursory Research for Embryonic Science and Technology (PRESTO), Japan Science and Technology Agency (JST), 4-1-8 Honcho, Kawaguchi, Saitama 332-0012, Japan

[4] Synchrotron Radiation Research Center, Kansai Photon Science Institute, Quantum Beam Science Research Directorate, National Institutes for Quantum and Radiological Science and Technology, Hyogo, 679-5148, Japan

[5] Resarch and Utilization Division, Japan Synchrotron Radiation Research Institute, Sayo-cho, Sayo-gun, Hyogo 679-5198, Japan

Keywords Synchrotron-radiation-based Mössbauer absorption spectroscopy · ^{61}Ni · Nuclear resonant scattering · Nanoparticles · Composites of nanoparticles · Metal-organic frameworks

1 Introduction

Ni is one of the most common elements. It is contained in various coins, superalloys, magnets, batteries, and so forth. It is also included in the human body and is a main component of the earth's core. Thus, it is a key element in physics, chemistry, biology, earth science, and other fields of science. It is also a group 10 element along with Pd and Pt, which show novel functionalities as catalyst and hydrogen storage materials. Thus, Ni and its compounds are expected to show novel functionalities similar to those of Pd and Pt. However, the functionalities of Ni compounds are inferior to those of Pd or Pt and are not sufficient in many cases. One possible way to enhance these functionalities of Ni compounds is to fabricate their nanoparticles. The electronic states of nanoparticles of a material are often considerably different from those of the bulk of the material and this difference sometimes yields a novel functionality. Furthermore, their electronic states are also affected by the surface coating materials. Recently, some researchers have attempted to control the electronic states proactively by using coating materials. Frameworks of metal complexes, which are called metal-organic framework (MOF), are sometimes used as the coating materials [1]. This type of composites of nanoparticles and MOFs are called nanoparticle/MOF composites. Many composites with Ni nanoparticles have also been synthesized [1–3]. Researchers expect charge transfer and/or other electromagnetic interaction between a nanoparticle constituent and a MOF constituent that will modify the electronic states of the nanoparticle constituent.

In these cases, it is essential to observe the electronic states of nanoparticles alone, although it is also difficult because the composites have two constituents, nanoparticles and MOFs. Fortunately, we can perform ^{61}Ni Mössbauer spectroscopy using radioactive isotope (RI) sources [4], which can observe the electronic states of Ni constituents, even when the sample includes two or more constituents including Ni. Furthermore, the time spectra of nuclear resonant forward scattering of synchrotron radiation (SR) by ^{61}Ni were successfully observed in 2007 and thus ^{61}Ni Mössbauer experiments using SR are also available in time domain [5]. Recently, SR-based Mössbauer absorption spectroscopy [6], by which we can obtain the energy spectra of nuclear levels similar to the established Mössbauer spectroscopy using RI, has also been made available. This method has already been applied to various Ni materials, such as a superconducting compound [7], a cathode in Li ion batteries [8], a Ni-substituted protein [9], and Ni nanoparticles [10]. Furthermore, this method is suitable for tiny amounts of samples because of the high brilliance of SR; many materials at the frontier of science are difficult to synthesize and thus this method is suitable for the study of such materials. The nanoparticle/MOF composites are an example of these materials and here we report the ^{61}Ni SR-based Mössbauer absorption spectroscopy of the composites.

2 Experimental

The MOFs used in our experiments were Ni-MOF-74, a MOF of the Ni_2(dhtp) complex; here, H_4(dhtp) is 2,5-dihydroxyterephthalic acid and thus the chemical formula of the MOFs was $Ni_2(C_8H_5O_6)$. The Ni nanoparticle/MOF composite sample was synthesized by partial thermal decomposition of Ni-MOF-74, in the same way as that reported in ref. [2]. In this

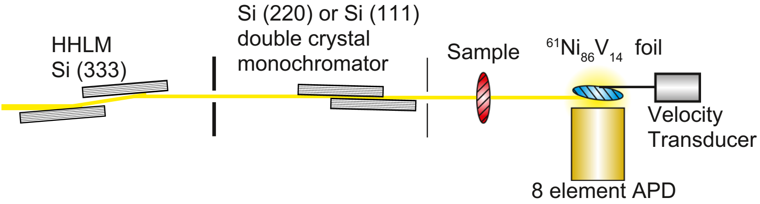

Fig. 1 Schematic drawing of the measurement system for ^{61}Ni SR-based Mössbauer absorption spectroscopy. The energy standard $^{61}Ni_{86}V_{14}$ foil and the detector were arranged in the same vacuum chamber to detect the internal conversion electrons

synthesis method, the MOFs were heated at 350 °C under vacuum for 12 h. During the heat treatment, the MOFs partially decomposed into Ni atoms and the atoms formed Ni nanoparticles. Thus, the composites were composed of Ni nanoparticles and the MOFs of Ni-MOF-74. The coexistence of nanoparticles and MOFs in the composites was confirmed by X-ray diffraction (XRD) and the nanoparticle constituent had a face-centered cubic (fcc) structure. According to ref. [2], the mean diameter of the nanoparticles must be 4.3 ± 1.4 nm and their composition must be $Ni_2(C_8O_6H_2){\cdot}9H_2O{\cdot}5Ni{\cdot}6C$. Furthermore, we also prepared a sample that was heated at 400 °C under vacuum for comparison. Under this condition, the MOFs were completely decomposed into Ni nanoparticles. These nanoparticles also had the fcc structure. According to ref. [2], the mean diameter of these completely decomposed nanoparticles must be 4.5 ± 1.4 nm and their composition must be $5Ni{\cdot}6C$.

The SR-based Mössbauer absorption spectroscopy experiments were performed at the undulator beamlines of SPring-8 (BL09XU: Public beamline for nuclear resonant scattering (NRS) experiments, and BL11XU: Contract beamline of National Institutes for Quantum and Radiological Science and Technology). The schematic drawing of the current measurement system for SR-based Mössbauer absorption spectroscopy is shown in Fig. 1. The operating modes of the storage-ring were several bunch modes at SPring-8: “203 bunch” mode, “406 bunch mode”, and “4 bunch train × 84” mode. The electrons in the storage ring were equally arranged in 203 bunches and the period of the bunches was 23.6 ns in the 203-bunch mode. They were equally arranged in 406 bunches and the period was 11.8 ns in the 406-bunch mode. The electrons were equally arranged into 84 groups, each of which consisted of four successive electron bunches in the 4 bunch train × 84 mode; the period of the groups was 57.0 ns and the interval of the successive bunches in a group was 1.97 ns [11]. The SR from the undulator was monochromatized to the energy of the first excited state of ^{61}Ni, 67.4 keV, by using a Si (333) high heat load monochromator (HHLM). Then it was transmitted to the Si double crystal monochromator to eliminate the low energy X-rays arising from the Si (111) reflection of HHLM. The index of the double crystal monochromator was (111) or (220). Then the SR passed through the samples. The samples were Ni-MOF-74, the completely decomposed Ni nanoparticles, and the nanoparticle/MOF composites. All samples were synthesized from natural Ni and the ^{61}Ni abundance was 1.14%. As for the Ni-MOF-74 sample, 179.4 mg of its powder was formed into a pellet with a diameter of 5 mm. As for the completely decomposed Ni nanoparticle sample, 205.3 mg of its powder was formed into a pellet with the same diameter. As for the composite sample, 192.0 mg of its powder was formed into a pellet with a diameter of 3 mm. The samples were cooled by a He-flow cryostat. The temperatures of the Ni nanoparticles and the composites were around 4 K and that of Ni-MOF-74 was around 6 K. Downstream of the sample, the SR was scattered by $^{61}Ni_{86}V_{14}$ polycrystalline foil. This alloy shows a simple single-line nuclear

Table 1 SR-bunch modes and time windows during the experiments of each sample

Sample	Bunch mode	Time window
Ni-MOF-74	203 bunch	3.9–19.5 ns
Ni nanoparticles after the complete decomposition	4 bunch train ×84	4.7–48.3 ns
Ni nanoparticle/MOF composite	406 bunch	5.6–9.1 ns

The time zero corresponds to the time of the irradiation of SR by each of the electron bunches except for the "4 bunch train × 84" mode. There were four electron bunches in a period in the "4 bunch train × 84" mode and the time zero corresponds to the time of irradiation of SR by the last, that is, fourth electron bunch in the bunch train in the period

resonant scattering profile down to 4 K and is sometimes used as the source material of RI ^{61}Ni Mössbauer spectroscopy [12, 13]. The enrichment of the $^{61}\mathrm{Ni}_{86}\mathrm{V}_{14}$ foil was 86.2%, its thickness was 3.1 ± 0.3 μm, and it was inclined 30° from the horizontal plane. The temperature of the foil was cooled to approximately 30 K by another He-flow cryostat at BL09XU or 40 K by a refrigerator at BL11XU. The nuclear resonant energy of this foil was controlled by a conventional velocity transducer that was connected to the foil. Therefore, this foil was the energy standard in this measurement system, that is, it determined the zero velocity. The frequency of the vibration of the transducer was 10–13 Hz. The emission from the foil was detected using an eight-element Si avalanche photo diode (APD) detector. The surface area of each element of the detector was 3 × 5 mm and its depletion layer was 150 μm in thickness. The detector was installed in the same vacuum chamber as the Ni-V foil to detect the internal conversion electrons as well as the directly scattered 67.4 keV γ-rays and fluorescent X-rays [14]. The NRS was counted in a time window after the irradiation of the SR pulse to the foil because NRS by ^{61}Ni was emitted with a delay (typically the lifetime of ^{61}Ni, 7.7 ns), while the electronic scattering occurred promptly. The time windows depended on the bunch mode and sample conditions, and are shown in Table 1. The dependence of the NRS intensity on the velocity of the foil was measured and we obtained the energy-domain Mössbauer spectra.

3 Results and discussion

The SR-based Mössbauer absorption spectra of the three samples are shown in Fig. 2. The counting rate of the NRS emitted from the Ni-V foil was 50–250 counts per second and the measurement time was 9–22.5 h. These spectra were analyzed by the formulae in the literature [6, 15, 16], using the following parameters [17]: the nuclear quadrupole moment of the ground state $Q_\mathrm{g} = +0.162$ barn, and that of the first excited state $Q_\mathrm{e} = -0.20$ barn, the nuclear magnetic moment of the ground state $\mu_\mathrm{g} = -0.75002\ \mu_\mathrm{N}$ (μ_N : nuclear magneton), and that of the first excited state $\mu_\mathrm{e} = +0.480\ \mu_\mathrm{N}$. In the analysis of the composites, we assumed that the composites possessed two components corresponding to the nanoparticle constituent and MOF constituent, and the MOF constituent showed the same Mössbauer parameters as those of the spectrum of only Ni-MOF-74. This was because the local environments of Ni were thought to be almost the same before and after the partial decomposition and the difference of the parameters between 4 and 6 K should be small. As discussed in the literature [10, 12, 13], the values of the isomer shift and quadrupole splitting in ^{61}Ni Mössbauer spectra are often very small and not as simple to use. Furthermore, there is no structural phase transition between the two temperatures. As for the magnetic

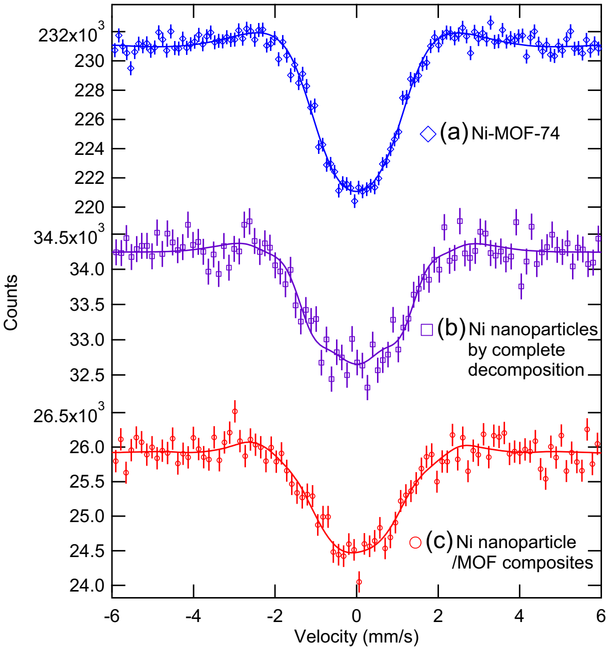

Fig. 2 ^{61}Ni SR-based Mössbauer absorption spectra. **a** Ni-MOF-74, **b** Ni nanoparticles by the complete decomposition of Ni-MOF-74, and **c** Ni nanoparticle/MOF composites

hyperfine field (MHF), the difference of the magnetization between 4 and 6 K was small (below 4%) from the magnetization measurement of Ni-MOF-74 [2] and thus the difference of MHF should also be small. The time window effect and the thickness effect were also taken into consideration for the analysis. We successfully evaluated the Mössbauer parameters under these assumptions, even for the composites, where both nanoparticle constituent and MOF constituent included Ni atoms. Figure 2 shows that the spectra showed shoulders on both sides of the absorption profiles. These arose from the time window effect, as discussed in ref. [15]. The time window also affected the linewidth. However, for the spectra in Fig. 2, the major contribution to the linewidth was the thickness of the samples. In fact, the ^{61}Ni thickness of the samples of the (a) Ni-MOF-74, (b) Ni nanoparticles, and (c) nanoparticle/MOF composites were 2.5, 9.6, and 15.2 mg/cm^2, respectively. If their recoilless fractions were similar to bulk Ni metal, the effective thicknesses corresponded to 2.8, 11, and 17, respectively. Thus, the spectra of (b) and (c) in Fig. 2 showed a broad line width.

The evaluated parameters are summarized in Table 2. As we expected, the isomer shifts and quadrupole splittings were almost zero within the experimental error. Therefore, we will concentrate on the MHF, henceforth. The MHF of the nanoparticles in the composites and that of the nanoparticles after the complete decomposition of MOFs were clearly different. Because the Ni nanoparticles in both samples had an fcc structure and their mean diameters were much the same, the difference arose from the surrounding MOFs. Because the lattice constants of the nanoparticles of both samples were similar, the difference in MHF meant that there were some interactions between the nanoparticle constituent and MOF constituent in the composites, such as charge transfer between them and the change of the arrangement of 3*d* and/or 4*s* electrons in the nanoparticle constituent.

Table 2 The Mössbauer parameters of the three samples evaluated from the spectra in Fig. 2

Sample		Isomer shift (mm/s)	Quadrupole splitting (mm/s)	Magnetic hyperfine field (T)
Ni-MOF-74		0.02 ± 0.02	0.02 ± 0.03	4.9 ± 0.1
Ni nanoparticles after the complete decomposition		−0.02 ± 0.05	0.0 ± 0.1	6.2 ± 0.3
Ni nanoparticle/ MOF composite	Nanoparticles[a]	−0.1 ± 0.1	0.3 ± 0.5	3 ± 1
	MOFs[a,b]	0.02[a]	0.02[a]	4.9[a]

The spectrum of Ni nanoparticle/MOF composites was analyzed with two components, corresponding to the nanoparticle constituent and the MOF constituent

[a] The area ratios of the constituents are approximately 3:2 for nanoparticles and MOFs

[b] The parameters of the MOF constituent in the composites sample were assumed to be the same as those of the Ni-MOF-74 sample

One possibility for this difference may be the simple increase of electrons in the 3*d* minor band of the nanoparticle constituent owing to the charge transfer from the surrounding MOF constituent. This situation reduced the MHF of the nanoparticle constituent through the decrease of the Ni atomic magnetic moments. This is a very simple model under the rigid band model. However, the XPS experiments in ref. [2] did not show clear charge transfer from the MOF constituent to the nanoparticle constituent and thus the electron transfer might be small. As for another possibility, the MHF of the Ni metal may also be reduced by the decrease of the 4*s* band electron density; in the nickel metal, the direction of MHF induced by the conduction band electrons is parallel to the direction of total MHF [18]. This might occur when the lattice of the nanoparticle constituent expands, although such an expansion was not observed in the XRD results. Therefore, we might have to consider changes beyond the rigid band model, that is, a slight modification of the band structure of Ni metal. If the simple slight charge transfer occurs, the degree of charge transfer to the nanoparticle constituent is expected to depend on the electronegativity of metals in the MOF constituent. Fortunately, many 3*d* transition metals form MOFs with organic complexes. A systematic study on the composites of Ni nanoparticles and MOFs including other metal ions will reveal the details of the possible charge transfer between nanoparticle the constituent and MOF constituent.

4 Summary

The SR-based Mössbauer absorption spectra of Ni-MOF-74, Ni nanoparticles after the complete decomposition of Ni-MOF-74, and the Ni nanoparticle/MOF composites were obtained. The Mössbauer parameters of the Ni nanoparticle constituent in the composites were successfully evaluated, although the Ni atoms were also included in the MOF constituent in the composites. We also succeeded in detecting the difference of the Ni nanoparticles and the Ni nanoparticle constituent in the composites; the MHF of Ni nanoparticle constituent in the composites is smaller than that of Ni nanoparticles after complete decomposition. Further systematic study on the composites of Ni nanoparticles and various MOFs will provide the detailed picture of the effect of the MOF constituent.

Acknowledgements The authors would like to thank the Accelerator Group of SPring-8 for their support, especially with the operation of several electron bunch-modes and the top-up injection operation. These experiments were performed at the BL09XU and BL11XU beamlines of SPring-8 with the approval of the Japan Synchrotron Radiation Research Institute (JASRI) (Proposal Nos. 2017A1862 for BL09XU, and 2015B3512, 2016A3508, 2017A3581 for BL11XU). A part of this work was performed under the Shared Use Program of Japan Atomic Energy Agency (JAEA) facilities (Proposal No. 2015B-E02) supported by JAEA advanced Characterization Nanotechnology Platform as a program of "Nanotechnology Platform" of the Ministry of Education, Culture, Sports, Science and Technology (MEXT). Another part of this work was performed under the Shared Use Program of National Institutes for Quantum and Radiological Science and Technology (QST) facilities (Proposal Nos. 2016A-E08 and 2017A-H01) supported by QST advanced Characterization Nanotechnology Platform as a program of "Nanotechnology Platform" of MEXT. A part of this work was supported by JSPS KAKENHI Grant-in-Aid for Scientific Research (S), Grant No. 24221005. We also thank Edanz Group (www.edanzediting.com/ac) for editing a draft of this manuscript.

References

1. Falcaro, P., Ricco, R., Yazdi, A., Imaz, I., Furukawa, S., Maspoch, D., Ameloot, R., Evans, J.D., Doonan, C.J.: Application of metal and metal oxide nanoparticles@MOFs. Coord. Chem. Rev. **307**, 237–254 (2016), for example. Many examples are reported in this review paper
2. Mukoyoshi, M., Kobayashi, H., Kudasa, K., Hayashi, M., Yamda, T., Maesato, M., Taylor, J.M., Kubota, Y., Kato, K., Takata, M., Yamamoto, T., Matsumura, S., Kitagawa, H.: Hybrid materials of Ni NP@MOF prepared by a simple synthetic method. Chem. Commun. **51**, 12463–12466 (2015)
3. Kobayashi, H., Mitsuka, Y., Kitagawa, H.: Metal nanoparticles covered with a metal-organic framework: from one-pot synthetic method to synergistic energy storage and conversion functions. Inorg. Chem. **55**, 7301–7310 (2016)
4. Obenshain, F.E., Wegener, H.H.F.: Mossbauer effect with Ni^{61}. Phys. Rev. **121**, 1344–1349 (1961)
5. Sergeev, I., Chumakov, A.I., Deschaux Beaume-Dang, T.H., Rüffer, R., Strohm, C., van Brück, U.: Nuclear forward scattering for high energy Mössbauer transitions. Phys. Rev. Lett. **99**, 097601 (2007)
6. Seto, M., Masuda, R., Higashitaniguchi, S., Kitao, S., Kobayashi, Y., Inaba, C., Mitsui, T., Yoda, Y.: Synchrotron-radiation-based Mössbauer spectroscopy. Phys. Rev. Lett. **102**, 217602 (2009)
7. Kishimoto, S., Nishikido, F., Haruki, R., Shibuya, K., Koshimizu, M.: Fast scintillation detectors for high-energy X-ray region. Hyperfine Interact. **204**, 101–110 (2012)
8. Segi, T., Masuda, R., Kobayashi, Y., Tsubota, T., Yoda, Y., Seto, M.: Synchrotron radiation-based ^{61}Ni Mössbauer spectroscopic study of $\mathrm{Li(Ni_{1/3}Mn_{1/3}Co_{1/3})}$ cathode materials of lithium ion rechargeable battery. Hyperfine Interact. **237**, 7 (2016)
9. Gee, L.B., Lin, C.-Y., Jenney, F.E. Jr., Adams, M.W.W., Yoda, Y., Masuda, R., Saito, M., Kobayashi, Y., Tamasaku, K., Lerche, M., Seto, M., Riordan, C.G., Ploskonka, A., Power, P.P., Cramer, S.P., Lauterbach, L.: Synchrotron-based nickel Mössbauer spectroscopy. Inorg. Chem. **55**, 6866–6872 (2016)
10. Masuda, R., Kobayashi, Y., Kitao, S., Kurokuzu, M., Saito, M., Yoda, Y., Mitsui, T., Hosoi, K., Kobayashi, H., Kitagawa, H., Seto, M.: ^{61}Ni synchrotron radiation-based Mössbauer spectroscopy of nickel-based nanoparticles with hexagonal structure. Sci. Rep. **6**, 20861 (2016)
11. SPring-8 website. http://www.spring8.or.jp/en/users/operation_status/schedule/bunch_mode (2017). Accessed 2 September 2017
12. Gütlich, P., Bill, E., Trautwein, A.X.: Mössbauer Spectroscopy and Transition Metal Chemistry. Springer, Berlin (2011)
13. Love, J.C., Obenshain, F.E., Czjzek, G.: Mössbauer spectroscopy with ^{61}Ni in nickel-transition-metal alloys and nickel compounds. Phys. Rev. B **3**, 2827–2840 (1971)
14. Masuda, R., Kobayashi, Y., Kitao, S., Kurokuzu, M., Saito, M., Yoda, Y., Mitsui, T., Iga, F., Seto, M.: Synchrotron radiation-based Mössbauer spectra of 174Yb measured with internal conversion electrons. Appl. Phys. Lett. **104**, 082411 (2014)
15. Seto, M., Masuda, R., Higashitaniguchi, S., Kitao, S., Kobayashi, Y., Inaba, C., Mitsui, T., Yoda, Y.: Mössbauer spectroscopy in the energy domain using synchrotron radiation. J. Phys. Conf. Ser. **217**, 012002 (2010)
16. Masuda, R., Kobayashi, Y., Kitao, S., Kurokuzu, M., Saito, M., Yoda, Y., Mitsui, T., Seto, M.: Synchrotron radiation based Mössbauer absorption spectroscopy of various nuclides. Hyperfine Interact. **237**, 43 (2017)
17. Bhat, M.R.: Nuclear data sheets for A=61*. Nuclear Date Sheets **88**, 417–532 (1999)
18. Wang, C.S., Callaway, J.: Energy bands in ferromagnetic nickel. Phys. Rev. B **15**, 298–306 (1977)